

COMPUTATIONAL MIRROR SYMMETRY

Andres Rios-Tascon



Cornell University

String Phenomenology Seminar 2022

Outline

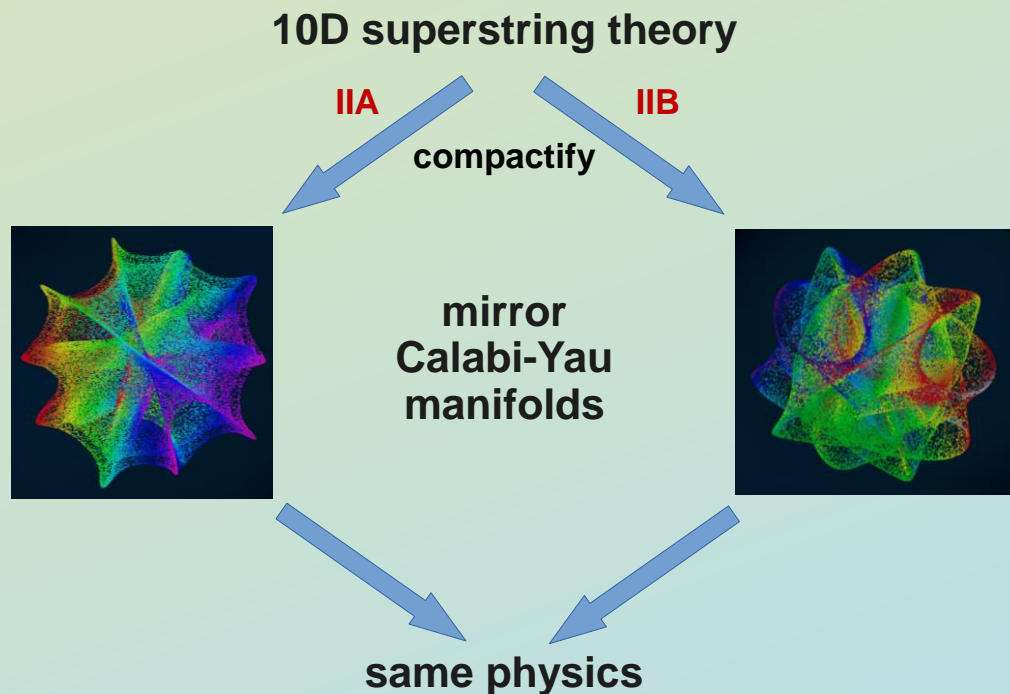
- Takeaways:**
- We made significant advancements in computing Gromov-Witten and Gopakumar-Vafa invariants, allowing us to study previously inaccessible parts of the landscape.
 - There are a wide range of phenomenologically interesting applications that we are beginning to explore.

Based on: M. Demirtas, M. Kim, L. McAllister, J. Moritz, A.R.T., work in progress

1. Motivation and background
2. Description of our advances
3. Insights and applications
4. Conclusions

Mirror Symmetry is a profound duality

Images: Geoffrey Fatin



Kähler moduli space \longleftrightarrow Complex structure moduli space
Complex structure moduli space \longleftrightarrow Kähler moduli space

Mirror Symmetry makes some hard problems easier

- Some computations can be done much more easily from a dual computation on the mirror Calabi-Yau.
- Candelas, De La Ossa, Green, and Parkes famously pioneered this approach by computing the number of rational curves in the quintic hypersurface in \mathbb{P}^4 , a known hard problem in algebraic geometry. [Candelas, De La Ossa, Green, Parkes '91]
- Today, I will talk about closely related topological invariants called genus-0 Gromov-Witten (GW) and Gopakumar-Vafa (GV) invariants.
- **Motivation:** GW/GV invariants provide powerful information about the geometry and tell us about non-perturbative contributions to the effective potential.

Relations from Mirror Symmetry

IIB on Calabi-Yau X

Complex structure “shape” moduli space

$$\mathcal{M}_{CS}(X)$$

$h^{2,1}$ -dimensional special Kähler manifold

Geometric interpretation as periods of the holomorphic 3-form Ω

$$\Pi := \begin{pmatrix} \int_{B^a} \Omega \\ \int_{A_a} \Omega \end{pmatrix} = \begin{pmatrix} \int_X \Omega \wedge \alpha_a \\ \int_X \Omega \wedge \beta^a \end{pmatrix} = \begin{pmatrix} \partial_{z^a} \mathcal{F} \\ z^a \end{pmatrix}$$

$\{A_a, B^a\}_{a=0}^{h^{2,1}}, (\{\alpha^a, \beta_a\}_{a=0}^{h^{2,1}})$ are symplectic basis of the middle (co)homology

z^a are projective coordinates

\mathcal{F} is prepotential of special geometry

Does not receive quantum corrections



IIA on Mirror Calabi-Yau \tilde{X}

Kähler “size” moduli space $\mathcal{M}_K(\tilde{X})$

$\tilde{h}^{1,1} = h^{2,1}$ -dimensional special Kähler manifold

Can construct analogous vector

$$\Pi := \begin{pmatrix} \partial_{t^a} \mathcal{F} \\ t^a \end{pmatrix}$$

t^a are complexified Kähler coordinates

\mathcal{F} is prepotential of special geometry

Receives α' corrections!

Match at Large Complex Structure (LCS)/large volume regimes and learn from the quantum corrections.

Let's go through the process in more detail

- Hosono, Klemm, Theisen and Yau (HKTY) devised an algorithmic procedure for Calabi-Yau hypersurfaces in toric varieties. We briefly recall the process.

[Hosono, Klemm, Theisen, Yau, hep-th/9308122, hep-th/9406055]

- Given a reflexive 4D polytope and its dual (Δ, Δ°) , we consider the CY hypersurface $f = 0$ in the properly desingularized toric variety given by the normal fan of Δ .
- From (integral) generators of the linear relations Q_i^a of Δ we can define gauge-invariant (local) coordinates

$$\tilde{\psi}_i \text{ are } h^{2,1} + 4 \text{ coefficients of } f \quad \psi_a := \prod_{i=1}^{h^{2,1}+4} \tilde{\psi}_i^{Q_i^a}, \quad a = 1, \dots, h^{2,1}$$

- The trick is to work in the Large Complex Structure (LCS) limit, construct a cycle $\Sigma_0 \in H_3(X, \mathbb{Z})$, and define a corresponding “fundamental period” as follows.

$$\omega_0 := \int_{\Sigma_0} \Omega = \frac{1}{(2\pi i)^4} \oint_{T^3} \oint_{f=0} \frac{d^4 s}{f}$$

Toric geometry is what enables us to pick an integral basis for the periods and compute the fundamental period.

Obtaining the period vector

- After some work one arrives at the following expression for the fundamental period.

$$\omega_0 = \sum_{\vec{n} \in \mathcal{M}_{\tilde{X}}} c(\vec{n}) \vec{\psi}^{\vec{n}} \quad \text{sum over curves in Mori cone } \mathcal{M}_{\tilde{X}}$$

- $c(\vec{n})$ vanishes for non-effective curves, so we can use $\mathcal{M}_{\tilde{V}} \supset \mathcal{M}_{\tilde{X}}$ since $\mathcal{M}_{\tilde{X}}$ is generally hard to compute.
- The periods of the CY satisfy a system of differential equations called the Picard-Fuchs equations. At LCS, the other periods can be found by taking derivatives of ω_0 .

$$\omega_0(\vec{\psi}, \vec{\rho}) := \sum_n c(\vec{n} + \vec{\rho}) \vec{\psi}^{\vec{n} + \vec{\rho}}$$

$$\omega^a := \frac{1}{2\pi i} \frac{\partial}{\partial \rho_a} \left(\omega_0(\vec{\psi}, \vec{\rho}) \right) \Big|_{\vec{\rho}=0}$$

are affine coordinates of the complex structure moduli space of X at LCS.

Matching with the mirror side

- The ω^a are matched with the Kähler coordinates $t^a, a = 1, \dots, h^{2,1}$. Thus, one can write

$$t^a = \frac{\log \psi^a}{2\pi i} + \frac{\alpha^a}{2\pi i}, \quad \alpha^a := \frac{1}{\omega_0} \sum_{\vec{n} \in \mathcal{M}_{\tilde{X}}} \left(\partial_{\rho_a} c(\vec{n} + \vec{\rho}) \right) \Big|_{\vec{\rho}=0} \vec{\psi}^{\vec{n}}, \quad \beta^{ab} := \frac{1}{\omega_0} \sum_{\vec{n} \in \mathcal{M}_{\tilde{X}}} \left(\partial_{\rho_a} \partial_{\rho_b} c(\vec{n} + \vec{\rho}) \right) \Big|_{\vec{\rho}=0} \vec{\psi}^{\vec{n}}$$

- Matching other entries in the period vector one finds quantum-corrected derivatives of the prepotential.

$$\partial_{t^a} \mathcal{F} = \underbrace{-\frac{1}{2} \tilde{\kappa}_{abc} t^b t^c + \tilde{a}_{ab} t^b + \frac{1}{24} \tilde{c}_a}_{\text{perturbative result}} - \underbrace{\frac{1}{(2\pi i)^2} \frac{1}{2} \tilde{\kappa}_{abc} (\beta^{bc} - \alpha^b \alpha^c)}_{\text{non-perturbative corrections to sigma model (in terms of } \psi^a)}$$

red values are topological data of \tilde{X}

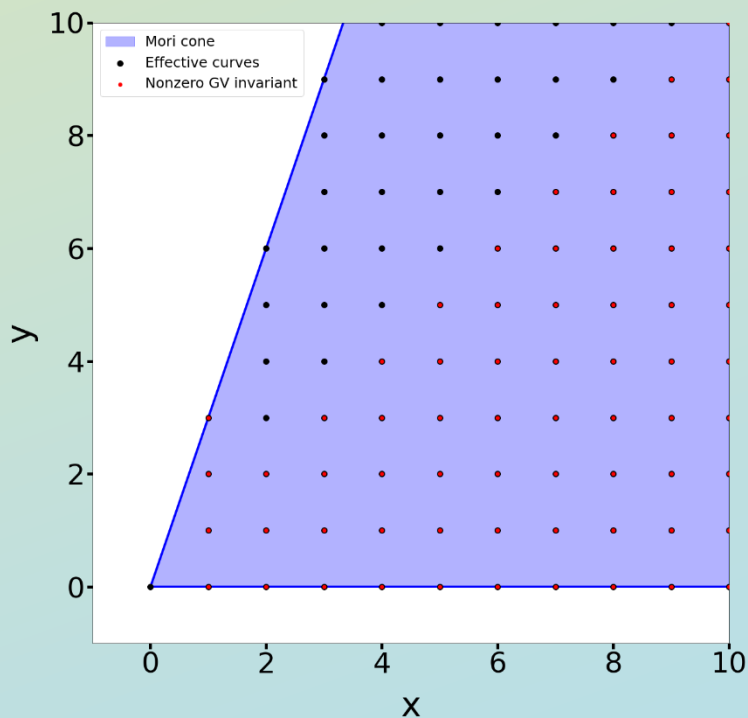
- One can rewrite the quantum corrections in terms of t^a to extract GW/GV invariants.

$$\frac{1}{2} \tilde{\kappa}_{abc} (\beta^{bc} - \alpha^b \alpha^c) = \sum_{\vec{n} \in \mathcal{M}_{\tilde{X}}} n_a \text{GW}_{\vec{n}} e^{2\pi i \vec{n} \cdot \vec{t}} = \sum_{\vec{n} \in \mathcal{M}_{\tilde{X}}} n_a \text{GV}_{\vec{n}} \text{Li}_2 \left(e^{2\pi i \vec{n} \cdot \vec{t}} \right)$$

GW versus GV

$$\sum_{\vec{n} \in \mathcal{M}_{\tilde{X}}} n_a \text{GW}_{\vec{n}} e^{2\pi i \vec{n} \cdot \vec{t}} = \sum_{\vec{n} \in \mathcal{M}_{\tilde{X}}} n_a \text{GV}_{\vec{n}} \text{Li}_2 \left(e^{2\pi i \vec{n} \cdot \vec{t}} \right)$$

- Both GW and GV invariants can only be non-zero for effective curves.





GW versus GV

$$\sum_{\vec{n} \in \mathcal{M}_{\tilde{X}}} n_a \text{GW}_{\vec{n}} e^{2\pi i \vec{n} \cdot \vec{t}} = \sum_{\vec{n} \in \mathcal{M}_{\tilde{X}}} n_a \text{GV}_{\vec{n}} \text{Li}_2 \left(e^{2\pi i \vec{n} \cdot \vec{t}} \right)$$

- Both GW and GV invariants can only be non-zero for effective curves.
 - GW invariants are rational and “count” the number maps from \mathbb{P}^1 into a curve class.
 - GV invariants are integer and are BPS indices $(n_V - n_H)$.
 - We will focus on GV invariants from now on for their integrality and more physical interpretation.
 - wrong intersection number
 - inconsistent truncation
 - missing effective curve
- } seemingly non-integral GV invariant

Very robust against computational mistakes!

Outline

1. Motivation and background 
2. Description of our advances 
3. Insights and applications
4. Conclusions

Existing tools for computing GV invariants

- Klemm wrote an influential Mathematica package called Instanton circa 1996.
- Kreuzer made some improvements to this package circa 2002. (Klemm, Kreuzer, Riegler, Scheidegger, [hep-th/0410018])
- These packages are still being used for recent papers.
(see e.g. Carta, Mininno, Righi, Westphal [2101.07272] and Carta, Mininno, Shukla [2112.13863])
- Instanton is a great package, but has a variety of shortcomings:
 - Limited to simplicial Mori cones
 - Cannot compute GV invariants of very high degree
 - Cannot study CYs with large number of moduli.

These limitations prevent us from studying most of the toric CYs we can construct!

We have extended the HKTY procedure and written new code to solve all these issues. Let's go through each of them.

Truncation scheme in Instanton

- Mori cones are assumed to be simplicial.
- Under this assumption, the degree of a curve is defined as follows.

$$c = \sum_{i=1}^{\tilde{h}^{1,1}} a_i e_i, \quad a_i \geq 0, \quad e_i \text{ generators of } \mathcal{M}_{\tilde{X}}, \quad \rightarrow \quad \deg(c) = \sum_{i=1}^{\tilde{h}^{1,1}} a_i$$

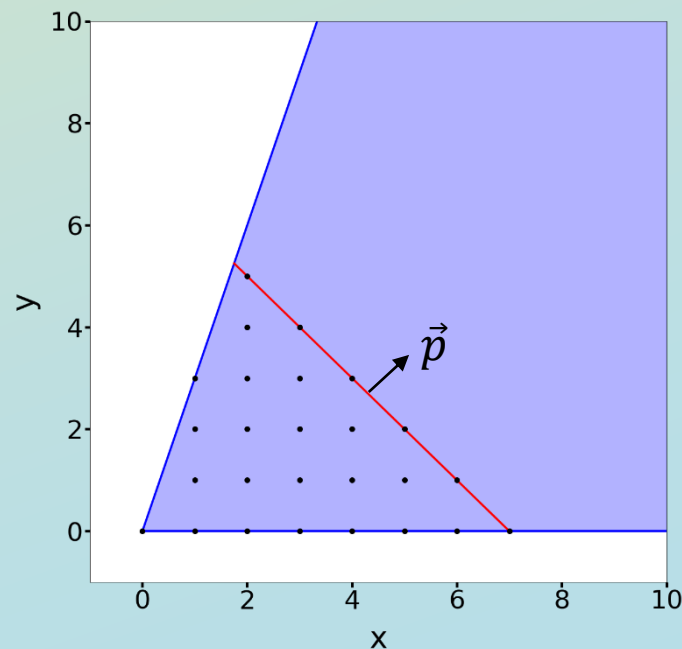
- The overwhelming majority of Calabi-Yau manifolds have a non-simplicial Mori cone.
- A workaround for this could be using a smooth cone that contains the Mori cone. However, this is extremely difficult and inefficient to do at large number of moduli.
- We devised a new truncation scheme that is more appropriate for non-simplicial Mori cones.

New Truncation Scheme

- Pick a point $\vec{p} \in \mathcal{K}_{\tilde{X}}$.
- We define the degree of a curve to be

$$\deg(\vec{c}) = \vec{c} \cdot \vec{p}, \quad \vec{c} \in \mathcal{M}_{\tilde{X}}$$

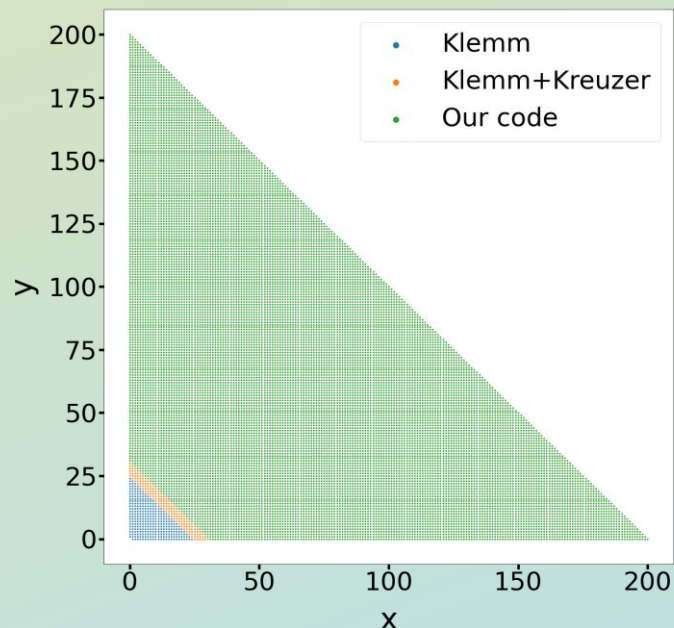
- Degrees are positive for non-zero effective curves.
- Truncation can be thought as given by a cutoff hyperplane defined by \vec{p} .
- Can be done even at large number of moduli.



Computing high-degree GV invariants

- We have written highly efficient C++ code that scales much better with degree and allows us to compute GV invariants up to much higher degree.

Example: hypersurface in $\mathbb{P}_{[1,1,1,6,9]}$ (2 moduli)

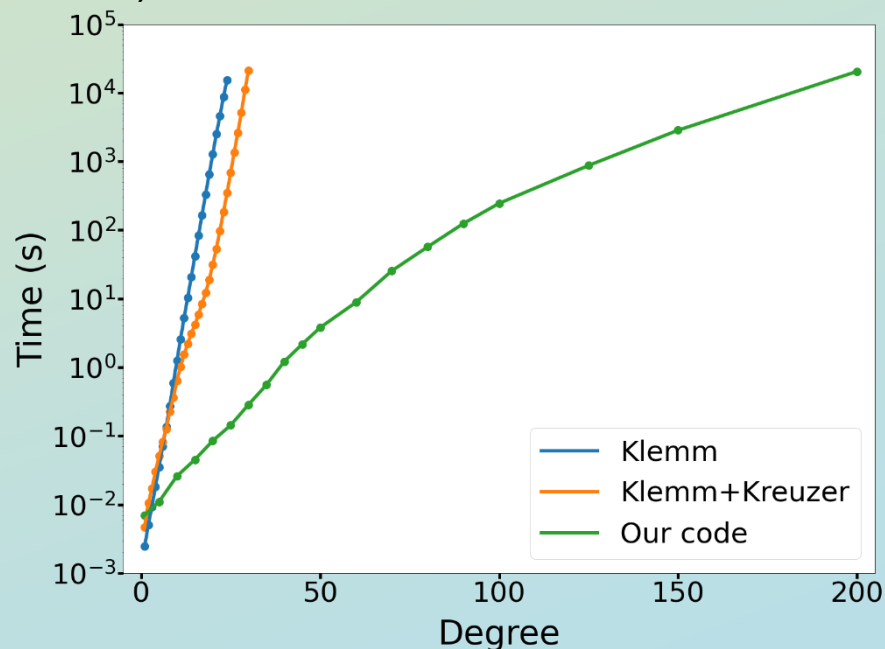
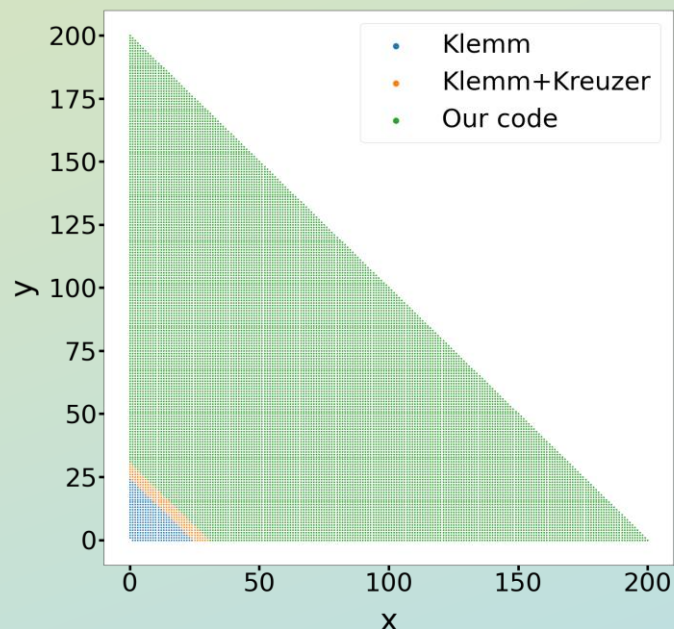


$$GV_{(43,157)} = \begin{aligned} &7262452829955349348898970729150141416679110693973320028351068818848 \\ &6432653251382058091815876545466225107920006052956233682847843384450 \\ &6024852438210575004841045244252519526429626073630184108775490151141 \\ &8496364363866593128124744924629990423053247956813814650497023692754 \\ &8171261686976659242173343606571934831950166806927881475472673536845 \\ &8166205443404677520894957842073350628815813666347835500521778963157 \\ &6603692419373884907789272751959442276020880914706818542923846400 \end{aligned}$$

Computing high-degree GV invariants

- We have written highly efficient C++ code that scales much better with degree and allows us to compute GV invariants up to much higher degree.

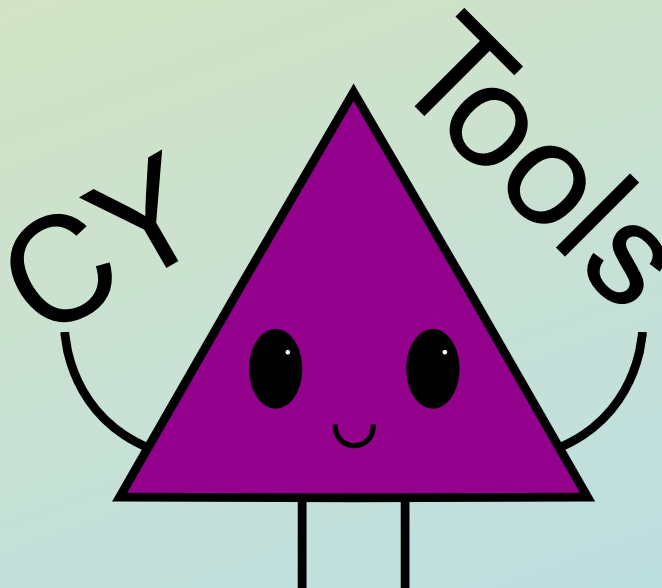
Example: hypersurface in $\mathbb{P}_{[1,1,1,6,9]}$ (2 moduli)



What about high degree AND large number of moduli?

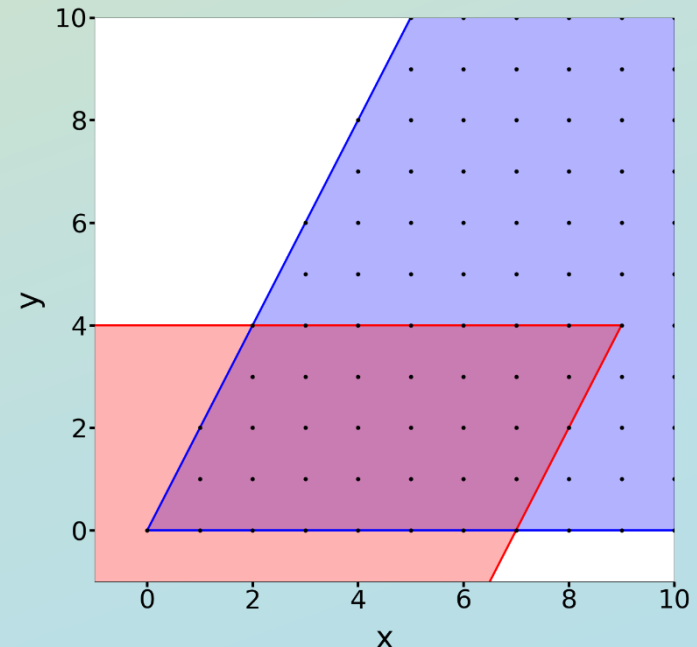
Exploring very large Hodge numbers

- A crucial ingredient is our CYTools package, which allows us to study any toric hypersurface CY in the Kreuzer-Skarke database. (Demirtas, McAllister, A.R.T. [2204.xxxxx])



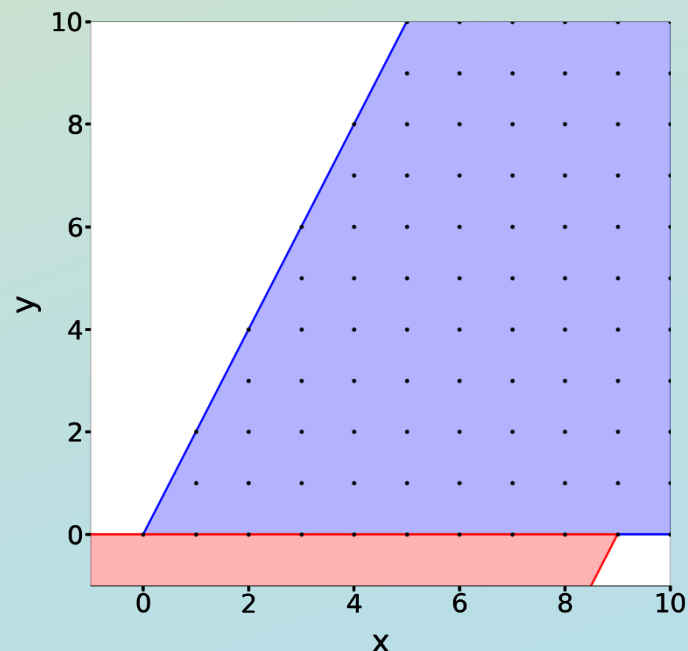
Exploring very large Hodge numbers

- A crucial ingredient is our CYTools package, which allows us to study any toric hypersurface CY in the Kreuzer-Skarke database. (Demirtas, McAllister, A.R.T. [2204.xxxxx])
- Computing GV invariants at very large Hodge numbers is still a hard task. However, we can use some tricks to our advantage.
- A key insight is that to compute the GV invariant of a curve one only needs information about curves in its “past light cone”.



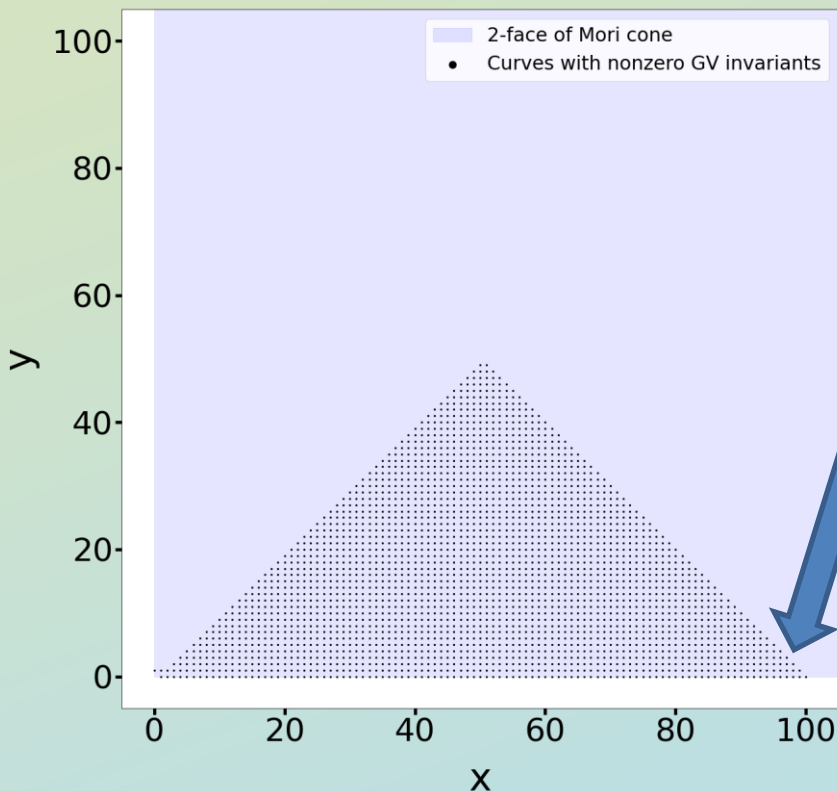
Exploring very large Hodge numbers

- A crucial ingredient is our CYTools package, which allows us to study any toric hypersurface CY in the Kreuzer-Skarke database. (Demirtas, McAllister, A.R.T. [2204.xxxxx])
- Computing GV invariants at very large Hodge numbers is still a hard task. However, we can use some tricks to our advantage.
- A key insight is that to compute the GV invariant of a curve one only needs information about curves in its “past light cone”.
- A special case happens when the curve lies on a face of the Mori cone, as only curves in that face need to be included.
- Computing GV invariants on an n -dimensional face, is roughly as difficult as computing GV for a CY with n moduli.



Example computation at very large number of moduli

Now let's look at a 2-face of the Mori cone of the mirror of the hypersurface in $\mathbb{P}_{[1,1,1,6,9]}$ we just looked at.

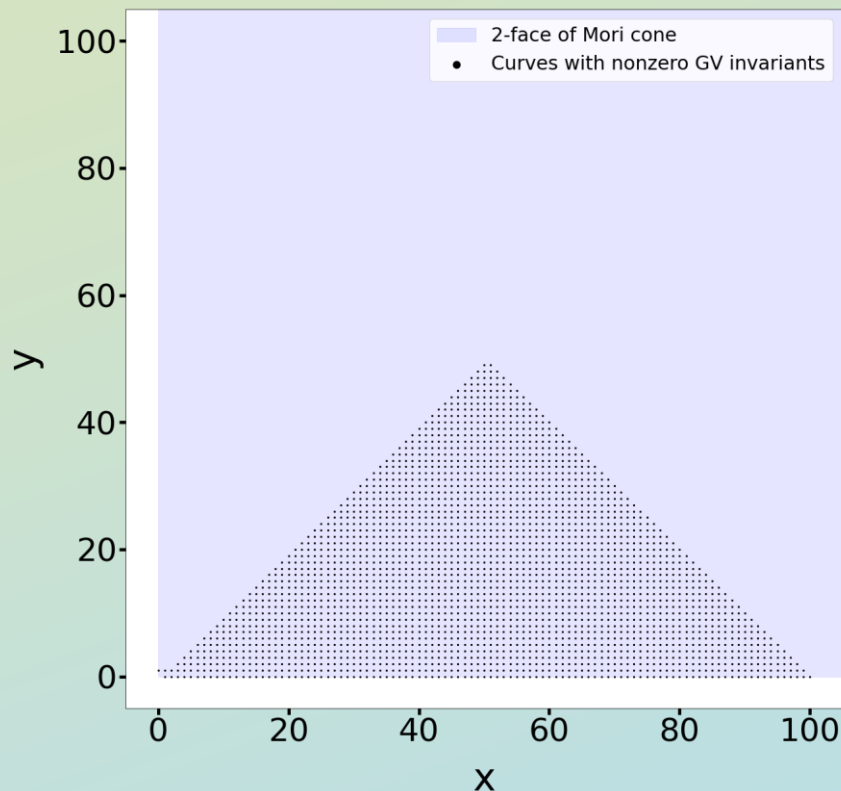


This is at 272 moduli!

$$GV_{\vec{n}} = \begin{matrix} -1612899483453220152528550546792414621795 \\ 19901273199675559622719699208469909604676 \\ 765613571656481821410846272619823538656 \end{matrix}$$

Example computation at very large number of moduli

Now let's look at a 2-face of the Mori cone of the mirror of the hypersurface in $\mathbb{P}_{[1,1,1,6,9]}$ we just looked at.



This is at 272 moduli!

When computing GV invariants at large number of moduli using the full-dimensional cone, we can obtain GV invariants of $\mathcal{O}(100K) - \mathcal{O}(1M)$ curves.

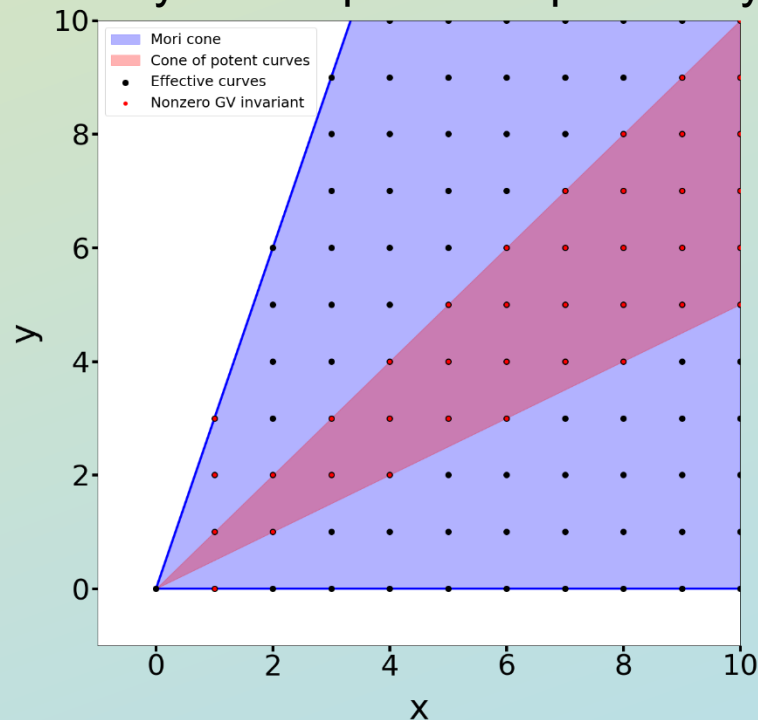
Our tools are not incremental improvements; they are game changers.

Outline

1. Motivation and background ✓
2. Description of our advances ✓
3. Insights and applications ←
4. Conclusions

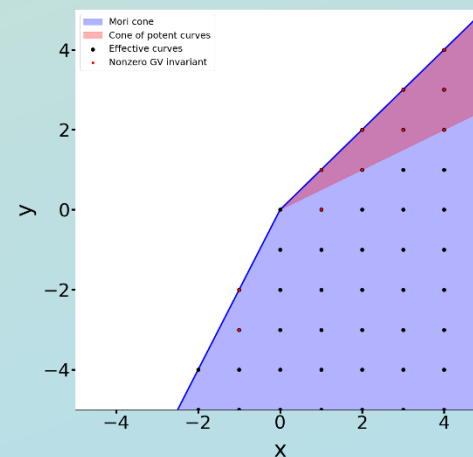
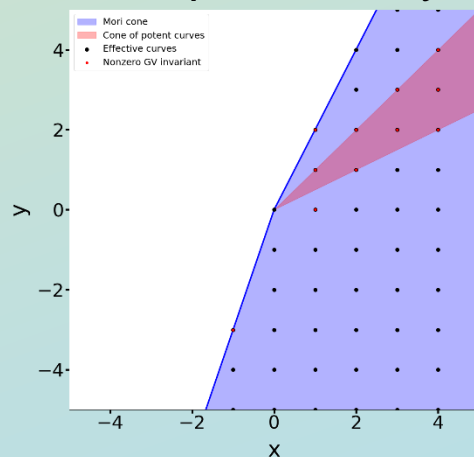
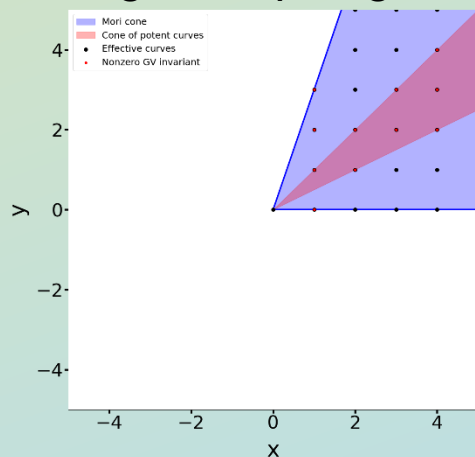
Insights from computing GV invariants

- The previous image gives us a glimpse at the way GVs are arranged:
 - There is a cone of potent rays (infinitely many non-zero GV invariants)
 - This cone is surrounded by a “bouquet” of nilpotent rays



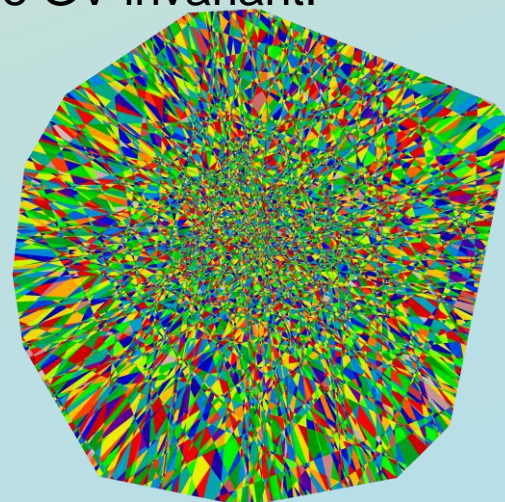
Insights from computing GV invariants

- The previous image gives us a glimpse at the way GV are arranged:
 - There is a cone of potent rays (infinitely many non-zero GV invariants)
 - This cone is surrounded by a “bouquet” of nilpotent rays
- At large number of moduli the cone of potent rays is very thin and there are many nilpotent rays. Thus, non-zero GV invariants are very sparse.
- Nilpotent extremal rays with positive GV invariants correspond to floppable curves, with non-extremal ones (potentially) being floppable curves in other phases. The change in topological data can be computed easily from the GV invariant.



Insights from computing GV invariants

- The previous image gives us a glimpse at the way GV invariants are arranged:
 - There is a cone of potent rays (infinitely many non-zero GV invariants)
 - This cone is surrounded by a “bouquet” of nilpotent rays
- At large number of moduli the cone of potent rays is very thin and there are many nilpotent rays. Thus, non-zero GV invariants are very sparse.
- Nilpotent extremal rays with positive GV invariants correspond to floppable curves, with non-extremal ones (potentially) being floppable curves in other phases. The change in topological data can be computed easily from the GV invariant.
- GV invariants thus allow us to explore non-toric phases and extended Kähler cones.
(c.f. Gendler, Heidenreich, McAllister, Moritz, Rudelius, upcoming)
- The numerous nilpotent rays and sparsity of non-zero GV invariants agree with the myriad of toric phases that we see. (c.f. Demirtas, McAllister, A.R.T. [2008.01730])



Applications of our advancements

- Potential math application: computing the exact Mori cone $\mathcal{M}_{\tilde{X}}$.
- Only effective curves can have non-zero GV invariants, so one might conjecture the following.

~~Conjecture: The Mori cone $\mathcal{M}_{\tilde{X}}$ is spanned by the curves with non-zero GV invariants.~~

- This conjecture is false because sometimes there are extremal rays with vanishing GV invariants. One might then propose a revised conjecture.

Revised conjecture: The Mori cone $\mathcal{M}_{\tilde{X}}$ is given by the smallest full-dimensional cone where the computation is consistent.

- So far this seems to be true, but more work needs to be done.

Pheno application: KKLT AdS with small c.c.

We made heavy use of GV invariants in our construction of KKLT AdS. We briefly recall an example we presented. (Demirtas, Kim, McAllister, Moritz, A.R.T. [2107.09064])

$$W_{flux} = W_{flux}^{(pert)} + W_{flux}^{(inst)} \sim 0 + \left[-2 \cdot \exp\left(2\pi i \tau \cdot \frac{7}{29}\right) + 252 \cdot \exp\left(2\pi i \tau \cdot \frac{7}{28}\right) + \mathcal{O}\left(\exp\left(2\pi i \tau \cdot \frac{43}{116}\right)\right) \right]$$

Use a choice of fluxes
such that $W_{flux}^{(pert)} = 0$

GV invariants

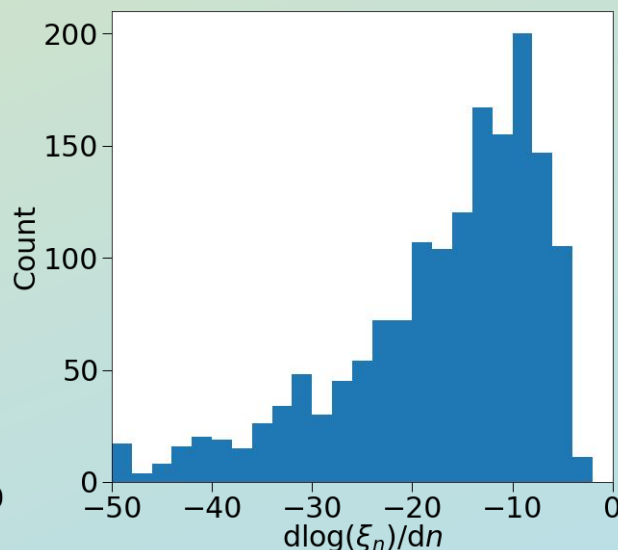
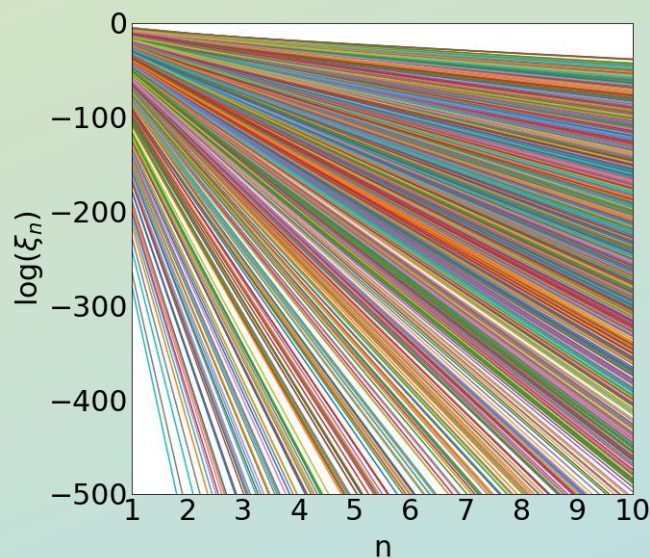
$$W_0 := \langle |W_{flux}| \rangle \approx 0.526 \times \left(\frac{2}{252} \right)^{29} M_{pl}^3 \approx 6.46 \times 10^{-62} M_{pl}^3$$

$$V_0 = -3M_{pl}^{-2} e^{\mathcal{K}} |W|^2 \approx -1.68 \times 10^{-144} M_{pl}^4$$

Checking our KKLT AdS

A key step is checking the validity of our construction was check the convergence of the series of (genus-0) worldsheet instanton corrections to the Kähler potential, which are the leading α' corrections.

Our constructions have large number of moduli, and we have to find potent rays to check the convergence.



$$\xi_n = GV_{n\vec{q}} e^{-2\pi n\vec{q}\cdot\vec{t}}$$

This kind of check would have been impossible to do with previous tools.

Other applications

- Tests for the Weak Gravity Conjecture (Gendler, Heidenreich, McAllister, Moritz, Rudelius, work in progress)
- Check for redundancies in KS database (c.f. Carta, Mininno, Righi, Westphal [2101.07272])
- Compute D7-brane superpotential (Kim, A.R.T., work in progress)
- Explore non-toric phases and infinite flop chains (c.f. Brodie, Constantin, Lukas, Ruehle 2104.03325)
- Probably many more that we have not thought about yet

Outline

1. Motivation and background



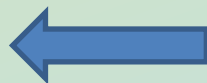
2. Description of our advances



3. Insights and applications



4. Conclusions

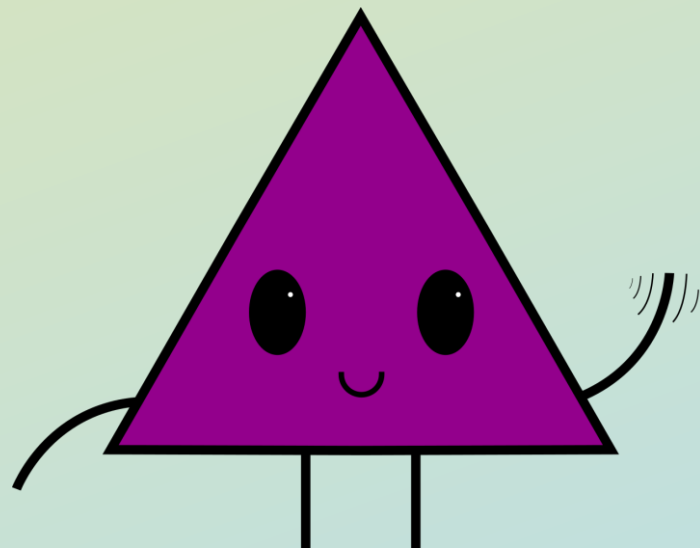


Conclusions

- We extended the HKTY procedure and wrote new code to compute GV invariants very efficiently.
- Our advancements enable us to study CYs that were far beyond the reach of any existing software.
- We developed these tools because we envisioned a wide variety of applications. We have started exploring some of these, but there are many more.
- Our new tools will eventually be integrated into our CYTools package, but we currently don't have a timeline for it.

If you have ideas and are interested in collaborating, then let's talk!

Thank you!



Questions?